Relaxation of Photogenerated Carriers in P3HT:PCBM Organic Blends

Thomas Moehl,[a] Vladimir G. Kytin,*[b] Juan Bisquert,*[a] Marinus Kunst,[c] Henk J. Bolink,[d] and Germà Garcia-Belmonte[a]

The after-pulse time-resolved microwave conductivity (TRMC) decays observed in P3HT:PCBM blends display a dependence on time close to $t^{-\beta}$, independent of excitation intensity, in the 10 ns–1 µs range. This is explained in terms of the relaxation of carriers in a Gaussian density of states (DOS). The model is based on a demarcation level that moves with time by thermal release and retrapping of initially trapped carriers. The model shows that when the disorder is large the after-pulse decay of the type $t^{-\beta}$ is obtained, while at low disorder and large temperature the carrier distribution becomes independent of time. In the measurements different β values were observed depending on the solvent used for spin-coating: 0.4–0.6 for chlorobenzene and 0.3–0.4 for toluene. The model was applied to extract the shape of the DOS from the TRMC decays, giving a dispersion parameter of about 120 meV for blends with high P3HT content.

1. Introduction

Bulk heterojunction (BHJ) solar cells comprise an interpenetrating blend of an optically active polymer and electron-accepting molecules.[1] BHJ organic solar cells have raised great interest towards the production of cheap and versatile photovoltaic (PV) devices; in particular the combination of poly(3-hexylthiophene) (P3HT) and [6,6]-phenyl C_{61}-butyric acid methyl ester (PCBM) has recently shown high photovoltaic performance[2] and stability.[3] In BHJ solar cells, excitons are generated by light absorption in the optically active polymer. These excitons dissociate at the polymer/molecule interface; spatially separating the electrons and holes which can then be transported to the electrodes by hopping. For improving the performance of BHJs, it is essential to understand and control the different steps that govern PV conversion.

Charge separation (exciton dissociation) and separate carrier transport through the mixed electron and hole conductor phases as well as recombination between the carriers in distinct phases are the major factors determining the production of photocurrent in the photoactive layer. It has been shown that P3HT:PCBM blends exhibit a remarkable improvement of performance when annealed, owing to better ordering of the polymer phase which enhances the hole conductivity.[4,5] Especially charge transport is a central issue because the mobility of charge carriers in organic conductors is generally very low.

Normally, carrier transport in organic conductors is greatly influenced by a wide distribution of traps that take the form of a Gaussian density-of-states (DOS).[6,7] Thus, a central parameter that determines the carrier conductivity is the dispersion parameter of the DOS σ_1, because this dispersion governs the field and density dependence of the mobility. Studies have shown that hole DOS dispersion varies from 70 meV for pristine P3HT[8] to broader values between 100 and 120 meV for P3HT:PCBM blends.[7] Several authors have described transport

in organic thin-film transistors (TFTs) using a multiple trapping model with the Gaussian DOS.[9,10] High hole mobilities ($\mu > 0.1\ \mathrm{cm^2 V^{-1} s^{-1}}$) have been obtained in P3HT samples in TFTs.[11]

It has been reported that the metal contacts in BHJ solar cell devices introduce important effects affecting device operation.[12] Therefore, contactless methods are an important tool for the analysis of the kinetics of photogenerated carriers and their dependence on the morphology of the blends. A number of studies have been presented by the contactless method of time-resolved microwave conductivity (TRMC).[13–15] Most of the studies have focused on the charge separation efficiency by the analysis of the maximum photoconductance signal at short times after the pulse, at varying incident light intensity.[13,16] Subsequent to the maximum response, monotonic after-pulse decay is observed. This decay is often adapted to a

[a] Dr. T. Moehl, Prof. J. Bisquert, Dr. G. Garcia-Belmonte
Photovoltaic and Optoelectronic Devices Group
Departament de Física, Universitat Jaume I
12071 Castelló (Spain)
Fax: (+34) 964 729 218
bisquert@fca.uji.es

[b] Dr. V. G. Kytin
Department of Physics
Moscow Lomonosov State University
119991, GSP-1, Moscow (Russia)
Fax: (+7) 095 939 1147
E-mail: kytin@mig.phys.msu.ru

[c] Dr. M. Kunst
Hahn-Meitner-Institut
Glienicker Str. 100
14109 Berlin (Germany)

[d] Dr. H. J. Bolink
Instituto de Ciencia Molecular
Universidad de Valencia
PO Box 22085, Valencia (Spain)

stretched exponential and has been attributed to spatial localization and trapping of separate electron and hole carriers;[17–19] however, a detailed model has not been developed yet.

In this work, TRMC measurements of blends with different P3HT:PCBM proportions will be analyzed and discussed. We present an interpretation of the after-pulse decay observed in terms of carrier relaxation in a broad density of states.

2. Results

We have studied blends of different ratios of P3HT and PCBM with weight fractions of P3HT between 90 to 100% and 1 to 10%. Some typical TRMC decays of these blends are presented in Figures 1, 2, and 3 in double logarithmic scale.
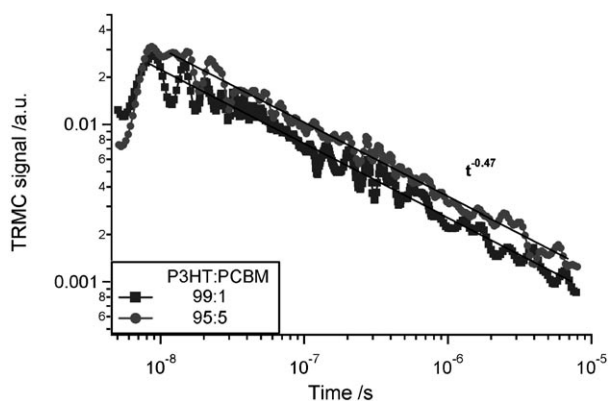
Figure 1. TRMC measurements of a 99:1 P3HT:PCBM (squares) and a 95:5 P3HT:PCBM (circles) blend with thicknesses of 140 and 160 nm, respectively, upon excitation by a 532 nm, 10 ns pulse (2.6×10^{16} photons cm^{-2} pulse^{-1}). The slopes of the decays are 0.47.
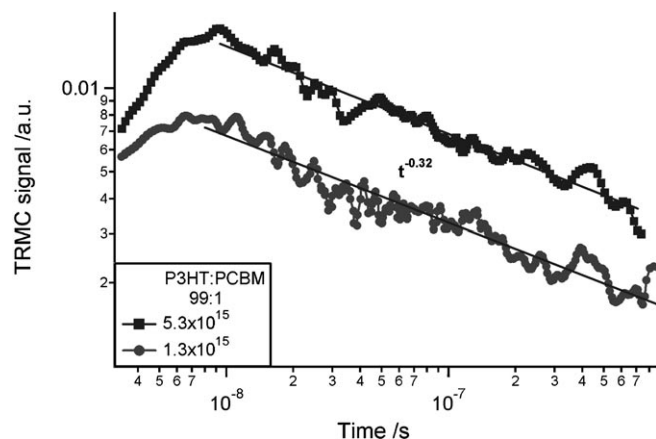
Figure 2. TRMC transients of a 99:1 P3HT:PCBM blend of 180 nm thickness spin-coated from a toluene solution (532 nm with light intensities of 5×10^{15} (squares) and 1.3×10^{15} photons cm^{-2} pulse^{-1} (circles)).

Figure 1 shows the microwave transient measurements of 99:1 and 95:5 P3HT:PCBM samples. The blends with concentrations of 1–10% of PCBM spin-coated from a chlorobenzene solution all show similar peak values of photoconductance upon excitation by the same light intensity. The decay of the photo-
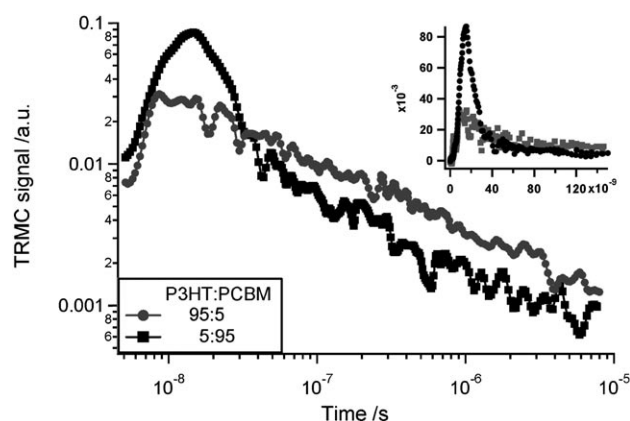
Figure 3. Comparison of TRMC transients of blends with 95% (circles) and 5% (squares) content of thiophene upon excitation with 2.6×10^{16} photons cm^{-2} pulse^{-1} at 532 nm. The inset shows the same data on a linear scale.

conductance exhibits a behaviour close to a power law $t^{-\beta}$, with the slope β in the range of 0.4 up to 0.6. Blends spin-coated from a toluene solution (Figure 2) show the lowest β (0.32) or, respectively, the slowest decay of the TRMC signal while the maximum photoconductance, compared to the blends spin-coated from chlorobenzene, stays unchanged. In Figure 2 one can also observe the dependence of the photoconductance peak on the photon density, which is observed in all of our blends with low PCBM content . It shows that the peak photoconductance (with light intensities between 10^{15} up to 10^{16} photons cm^{-2} pulse^{-1}) exhibits a sublinear dependency on light intensity. This indicates a recombination of higher order during the laser pulse itself.

In general all of these blends show a decay kinetic nearly independent of light intensity, which is in agreement with results obtained by Savenije et al. for blends of PCBM and a poly-(phenylene vinylene) (PPV:PCBM) with less than 60% PCBM.[14]

If the content of PCBM is strongly increased, the shape of the decay behaviour changes notably. Figure 3 shows a comparison of the TRMC signal of blends with a composition of 95:5 and 5:95 P3HT:PCBM illuminated with the same photondensity. The initial photoconductance peak increases strongly if the content of PCBM is high. A new fast decay process appears showing a steep slope of the initial photoconductance signal with a $\beta \sim 2$.

3. Model

The investigation of the kinetics of the decay of excess charge carriers by TRMC involves the measurement of the excess conductivity $\Delta\sigma(t)$ induced by an external stimulus as a function of time. The parameter $\Delta\sigma(t)$ can be determined from the change in the reflected microwave power, $\Delta P(t)$. For small perturbations, the TRMC signal, $\delta U = \Delta P / P_{in}$ (P_{in} is the incident microwave power), is proportional to the induced conductivity $\delta U = -A\Delta\sigma$ with A, a sensitivity factor, accounting for setup and conditions of the measurements. An introduction to this technique and its application to dispersive transport in inorganic

semiconductors such as a-Si:H can be found in earlier work by Kunst and Werner.[20]

The idea is now to adopt the classical interpretation of photoconduction transients based on a demarcation level that shifts with time because of carrier release and retrapping[21,22] from a transport level[23] and corresponding relaxation of charge carriers, and apply it to the TRMC transients of blends with low content of PCBM.

For an exponential distribution, it is well-known[21,24] that this approach implies a decay of the photoconductance of the type $t^{\alpha-1}$, with $\alpha = T/T_0$ being the coefficient of dispersive transport (with T the temperature and T_0 the depth of the distribution). We will point out the differences that occur when the DOS is a Gaussian, as usually found in organic conductors,[6] and discuss the experimental results in terms of this model. A theoretical simulation of the demarcation level shifts of holes with time in a Gaussian DOS is exemplified in Figure 4 using the model further explained below.

Time-dependence of photoconductivity. The model follows the classical derivation for the relaxation of carriers photogenerated by a light pulse.[21,24] In brief, the charge carrier distribution is approximately given by the Fermi function with time

(a)

(b)
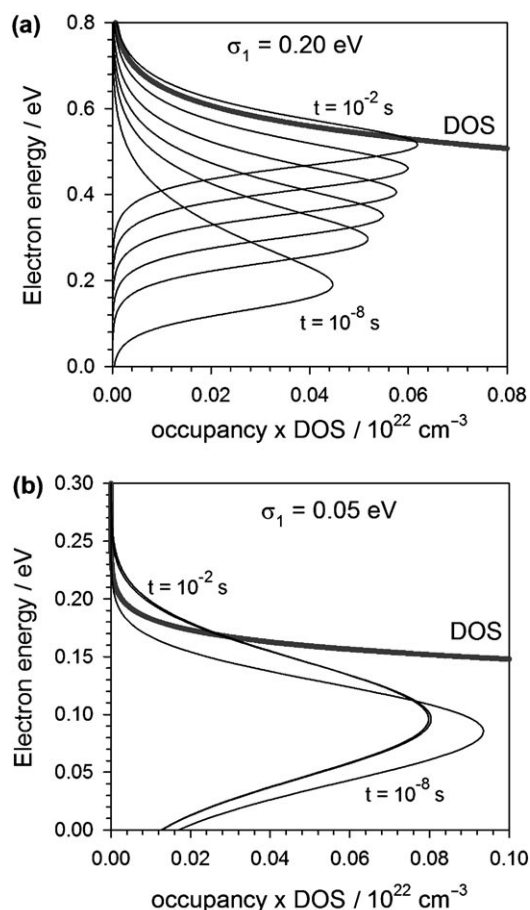
Figure 4. Simulation of the evolution of hole carrier density in a Gaussian distribution centred at $E = 0$ eV and with disorder parameter as indicated, following photoexcitation, at time intervals differing by a factor 10 from 10^{-8} to 10^{-2} s. Parameters used in the simulation: $T = 300$ K, $N_L = 10^{22}$ cm^{-3}, $N_{tr} = 10^{22}$ cm^{-3}, $p_0 = 10^{20}$ cm^{-3}, $\nu_0 = 10^{12}$ s^{-1}.

dependent quasi Fermi level and time dependent pre-factor. We assume that the carriers are holes (as discussed below) in the Gaussian DOS given by

$$g(E) = \frac{N_1}{\sqrt{2\pi}\sigma_1} \exp\left[-\frac{(E - E_1)^2}{2\sigma_1^2}\right] \qquad (1)$$

where N_1 is the total density of localized states, E_1 is the centre of the distribution, and σ_1 is the width. We also assume that the capture coefficient is the same for all traps,[22] hence, the DOS is initially populated uniformly above the transport energy E_{tr}. After a time t, the shallow states release and retrap holes a large number of times, so that these states effectively obtain a thermal distribution. The demarcation energy level $E_d(t)$ below which holes are released at time t is determined by Equation (2).

$$t = \nu_0^{-1} \exp[(E_d(t) - E_{tr})/k_BT] \qquad (2)$$

where k_B is the Boltzmann constant. The demarcation shifts up with time, as shown in Figure 4a, depopulating the states below $E_d(t)$ and adding more trapped charge to the states above $E_d(t)$ in addition to the frozen-in charge that is already present, so that the total density of excess carriers remains constant. Because the occupation number below $E_d(t)$ is energy-independent and decays exponentially with energy above $E_d(t)$, the distribution of holes is approximately described by[24]

$$p(E, t) = \phi(t)g(E)F[E, E_d(t)] \qquad (3)$$

in terms of a time-dependent occupancy factor $\phi(t)$ that ensures that the initial excitation is conserved, and the Fermi-Dirac distribution function is

$$F(E, E_d(t)) = \frac{1}{1 + e^{(E - E_d(t))/k_BT}} \qquad (4)$$

The conservation of carriers can be stated as

$$\phi(t) \int_{-\infty}^{\infty} g(E)F[E, E_d(t)]dE = p_0 \qquad (5)$$

and the density of holes in the transport level is given by

$$p(t) = N_{tr}\phi(t)e^{[E_{tr} - E_d(t)]/k_BT} \qquad (6)$$

where $N_{tr} = g(E_{tr})k_BT$ is the effective amount of states at the transport level.

Shape of the decays. Simulations of the decay of photogenerated carriers at different temperatures and for different values of the disorder parameter σ_1 are shown in Figure 5. In an exponential DOS the decay is given by a power law, as mentioned previously, and this is nearly the case also in some conditions in the Gaussian DOS, as observed in the simulations of Figure 5. However, a different behaviour is found when the
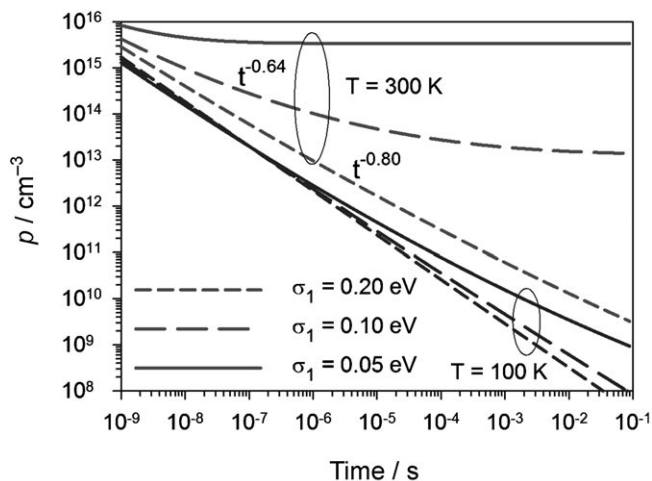
Figure 5. Simulation of the decay of hole carrier density at the transport level following photoexcitation, at two different temperatures, and for varying disorder parameters as indicated. Parameters used in the simulation: $N_L = 10^{22}$ cm^{-3}, $N_{tr} = 10^{22}$ cm^{-3}, $E_{tr} = 0.1$ eV, $p_0 = 10^{20}$ cm^{-3}, $\nu_0 = 10^{12}$ s^{-1}. The fits to $t^{-\beta}$ dependence shown correspond to the linear part of the curves at short times.

temperature is high and the broadening of the DOS is small. In that case the photoconductance decays only for a limited time period that gets shorter with a decreasing disorder parameter σ_1, and thereafter it remains constant. This behaviour is well-explained by the properties of the carrier distribution in a Gaussian DOS.[6] For a thermalized distribution of holes, it is well-known that the carriers form a Gaussian distribution of width σ_1 centered at the energy level E_m, independent of the Fermi level E_{Fp},[6] provided that the Fermi level is high, that is, $E_{Fp} > E_m$, being

$$E_m = E_1 + \frac{\sigma_1^2}{k_B T} \tag{7}$$

Therefore, the decay becomes constant when $E_d(t) \approx E_m$, because the demarcation level effectively stops at E_m and the hole density becomes stationary. The fact that the distribution becomes stationary is appreciated in Figure 4(b). In contrast to this, at low temperatures, E_m lies very high and the decay of the hole density appears as a power law, as already mentioned.

Calculation of the shape of the DOS. Equations (5) and (6) can be used to extract the shape of DOS from the TRMC signal δU, which is proportional to the hole density at the transport energy level:

$$\delta U = B\phi(t)\exp\left(\frac{E_{tr} - E_d(t)}{k_B T}\right) = C\frac{\phi(t)}{t} \tag{8}$$

where B and C are time-independent constants determined by experimental conditions. Therefore, transient photoresponse can be used for determination of the shape of the DOS. The integral in equation (5) can be taken in parts and then expanded in a series:

$$\int_{-\infty}^{\infty} \frac{g(E)dE}{\exp\left(\frac{E_d(t)-E}{k_B T}\right) + 1} =$$

$$- \int_{-\infty}^{\infty} \frac{1}{\exp\left(\frac{E_d(t)-E}{k_B T}\right) + 1} d\int_E^{\infty} g(E')dE' =$$

$$\frac{1}{kT} \int_{-\infty}^{\infty} \frac{\exp\left(\frac{E_d(t)-E}{k_B T}\right)}{\left(\exp\left(\frac{E_d(t)-E}{k_B T}\right) + 1\right)^2} = \int_E^{\infty} g(E')dE' =$$

$$= \int_{-\infty}^{\infty} \frac{\exp(x)}{(\exp(x) + 1)^2} = \int_{E_d(t)-k_B Tx}^{\infty} g(E')dE' dx$$

$$\approx \int_{E_d(t)}^{\infty} g(E)dE + \sum_{n=1}^{\infty} \frac{(-1)^{n+1}}{n!}(kT)^n g^{(n-1)}(E_d(t)) \int_{-\infty}^{\infty} \frac{x^n \exp(x)dx}{(\exp(x) + 1)^2} \tag{9}$$

Because the accuracy of energy determination in the demarcation level concept is $k_B T$, we can take only the first term in this series and we get

$$\int_{-\infty}^{\infty} \frac{g(E)dE}{\exp\left(\frac{E_d(t)-E}{kT}\right) + 1} \approx \int_{E_d(t)}^{\infty} g(E)dE \tag{10}$$

and therefore

$$\delta U \approx \frac{Cp_0}{t \int_{E_d(t)}^{\infty} g(E)dE} \tag{11}$$

Taking into account that

$$\frac{d}{dE_d(t)} = \frac{d}{d(k_B T \ln t)} \tag{12}$$

we obtain from Equation (11) the following expression for determination of the shape of DOS from TRMC signal:

$$g(k_B T \ln t) = -Cp_0 \frac{d}{d(k_B T \ln t)}\left(\frac{1}{t\delta U}\right) \tag{13}$$

4. Discussion

Concerning the sign of the carriers responsible for the observed decay, the TRMC method cannot distinguish between holes and electrons and therefore normally $\Delta\sigma(t)$ is dominated by the charge carrier which possesses the higher mobility. In literature there exist a wide range of determined values for the mobility of holes and electrons in pristine materials and blends determined by different techniques such as time-of-flight (TOF), current density-voltage curves, pulse-radiolysis, and flash-photolysis TRMC. Some reports claim that the electron mobility in PCBM exceeds the hole mobility in P3HT (the latter approximately equal to 2×10^{-3} cm^{2}V^{-1}s^{-1}) by at least one

order of magnitude.[5] However, Dicker et al.[13,17] report a measured mobility of holes at 0.014 cm²V⁻¹s⁻¹ in P3HT using TRMC, and in TFT measurements mobility values for P3HT as high as 0.1–0.5 cm²V⁻¹s⁻¹ have been found.[9,11] These discrepancies of determined mobility values originate presumably from different chemicals used, different sample preparation methods and post-treatments, and surely to some extent from the applied technique. Doubtless, the mobility of the charge carriers in these blends changes with composition of the polymer/fullerene mixture due to the different resulting morphologies.[15]

Therefore, to monitor exclusively the microwave decay of the holes in P3HT, blends of low PCBM proportion (1–10%) were prepared and investigated. It is assumed that at this low content of fullerene (<20%), after excitation and charge separation at the heterojunction, isolated fullerene anions are embedded in a polymer matrix and represent a localised electron that can not contribute to the light-induced conductivity change of the measured samples.[14] Even at this low PCBM content, high exciton dissociation at the polymer/fullerene interface is achieved and the yield of generated holes is about 75% (in comparison to 2% for the pristine polymer), comparable to light harvesting in a complete organic solar cell device.[16]

In our blends with high PCBM concentration (>90%) we can observe a different decay behaviour with the slope $\beta \sim 2$. As mentioned above, the photoconductance peaks are higher and show a faster decay. The origin of the fast decay process is yet unclear but at this high PCBM content several additional effects influence the absorption and charge generation and therefore the decay behaviour (e.g. the absorption of the PCBM in the visible range or generation of more than one charge carrier per particle). With the slope $\beta \sim 2$ presumably several different processes, such as exciton–exciton annihilation and direct electron–hole recombination, contribute to the measured decay signal, giving this high slope.

In literature, the TRMC decay of blends with low PCBM content is also interpreted as a recombination process between electron and holes, giving similar slopes for the power law decay.[16] Because we have observed,[12] in solar cells prepared with this type of blends, that the recombination lifetime is of the order of 100 µs, the decrease of the carrier density by recombination should become notable at longer times than those considered in, for example, Figure 1. In consequence we will assign the after-pulse decays with power law time-dependence, observed in Figure 1 and 2, to the reorganization of the holes injected into a Gaussian DOS by exciton dissociation.

Figure 6 shows the results for the extraction of the shape of DOS from TRMC decays using Equation (13). To suppress the noise we took the required derivatives by linear fit averaging of the dependence of $(t\,\delta U)^{-1}$ on $(k_B T \ln t)$ at the energy interval $k_B T$ at each point. As can be seen the DOS shape in the films is close to exponential in the available energy range. In the film with 99% P3HT from Figure 1 it is impossible to see the negative curvature of the shape of DOS presented in semilogarithmic scale and determine the width σ_1 of Gaussian DOS. This is, however, possible for the films with 95%, as indicated
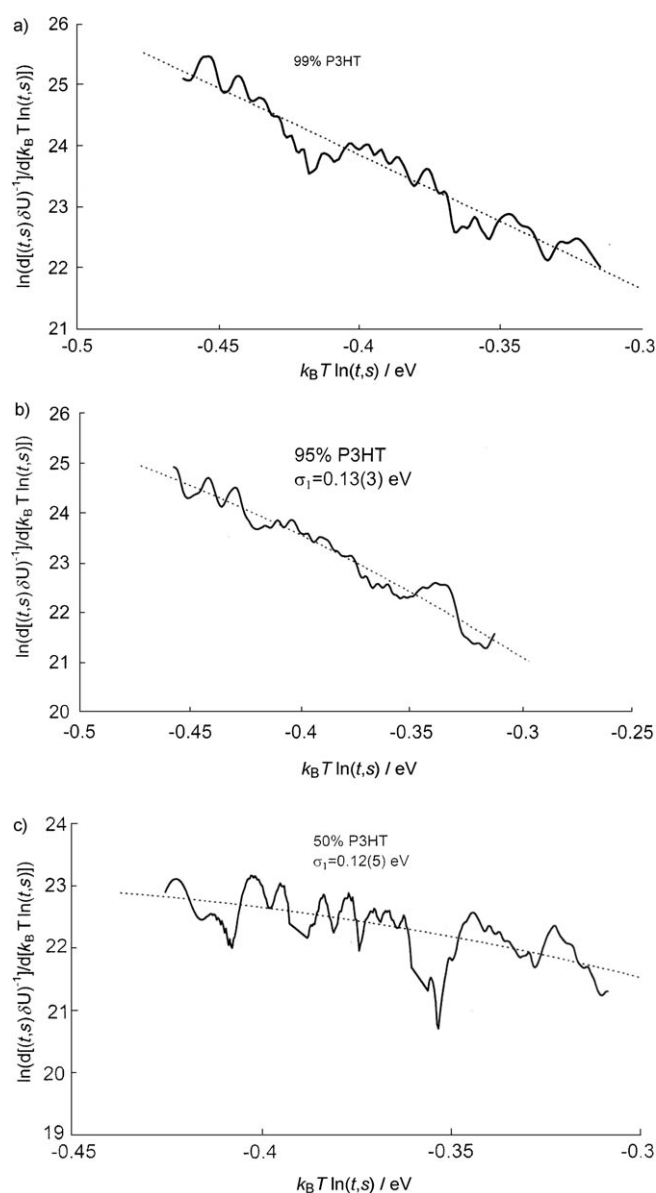
Figure 6. The shape of DOS and corresponding DOS parameters extracted from TRMC decay using Eq. (13) for the blends with a) 99% P3HT, b) 95% P3HT, and c) 50% P3HT.

in Figure 6 b). The extraction of σ_1 for a 50% P3HT sample gives a comparable value (Figure 6 c). The obtained estimate of DOS width is quite large, about 120 meV, in agreement with previous results.[7] Correspondingly, the width of DOS for the film with 99% P3HT must be larger.

Our interpretation is in agreement with previous TOF measurements of conjugated polymers (polyphenylenevinylene-ether)[25] that were also explained in terms of the relaxation of carriers in a Gaussian DOS. In TOF experiments at high temperature the equilibrium is established rapidly and a plateau of conductivity is observed. In contrast to this, at low temperature the thermalization is slower than the transit time, and dispersive transport is obtained.[26] This is similar to the behaviour described in Figure 5. Comparable results have been obtained using photoinduced charge carrier extraction techniques.[27] Al-

ternative, important evidence for charge carrier relaxation was found by Durrant et al. using transient absorption spectroscopy.[28,29] They observed power law decays in dialkoxy-phenylene-vinylene polymer (MDMO-PPV:PCBM) blends and attributed them to carrier dynamics in a tail of localized states.

We have shown that it is plausible to interpret the transients of TRMC in organic blends over several time decades in terms of reorganization of (hole) carriers in a Gaussian DOS, and subsequently to obtain the shape of the DOS by deconvolution of the TRMC decays. However, further description of the data must take into account a number of important aspects. (i) Carrier relaxation can occur by hopping between the localized levels.[30] Also high-frequency hole (electron) long-range transport can occur by either hopping or band transport. (ii) The TRMC can also correspond to bound carriers, by the polarizability of the localized states filled with holes (electrons).[31] (iii) Some concepts of trap-limited recombination provide the decay law $t^{-\beta}$ but with a different temperature dependence.[22,32] Work to consider these additional effects for a more complete interpretation of the data is in progress.

Conclusions

We investigated spin-coated blends of P3HT and PCBM with low (<10%) and high (>90%) content of PCBM with TRMC measurements and observed two different decay behaviors for the different compositions. The decays of samples containing more than 90% PCBM were not further interpreted because the processes involved are unknown so far. The decay of the samples containing low proportions of PCBM showed different slopes depending on the solvent used for the spin-coating (0.4–0.6 for chlorobenzene and 0.3–0.4 for toluene). We could show that the TRMC decay of P3HT:PCBM blends with low content of PCBM can be interpreted in terms of the reorganization of holes in a Gaussian shaped DOS giving valuable information about transport and blend properties. Understanding the factors which determine these properties and how they affect the overall performance of a BHJ solar cell is crucial to further increase the efficiency of such devices.

Experimental Section

The blends of P3HT and PCBM were, if not indicated otherwise, spin-coated from a chlorobenzene solution on quartz glass substrates in ambient conditions and kept thereafter under vacuum until the measurements were performed. The resulting films had thicknesses of 100 to 200 nm. No post-treatments such as thermal annealing were performed on the films. Contactless transient photoconductance measurements were performed in the microwave range via TRMC. The microwaves were generated by a Gunn diode (30 GHz, K_a-band) and transmitted by a waveguide via circulator to the sample, which was positioned on the outlet of the waveguide. The fraction of the microwave power reflected by the sample was separated by passing the circulator. The reflected microwave power was detected with a Hewlett-Packard HP R422C which was connected to a digitizer (TDS Tektronix 620B). Excitation of the sample came from a Nd:YAG laser giving a 10 ns laser pulse (~ 20 mJ cm^{-2}; ~ 5.36 × 10^{16} photons cm^{-2} pulse^{-1}) with a repetition frequency of 10 Hz. The wavelength used for the excitation was 532 nm from the second harmonic of the laser. A more detailed description of the setup can be found elsewhere.[33]

[1] C. J. Brabec, N. S. Sariciftci, C. Hummelen, *Adv. Funct. Mater.* **2001**, *11*, 15.

[2] W. Ma, C. Yang, X. Gong, K.-S. Lee, A. J. Heeger, *Adv. Funct. Mater.* **2005**, *15*, 1617.

[3] J. A. Hauch, P. Schilinsky, S. A. Choulis, R. Childers, M. Biele, C. J. Brabec, *Sol. Energy Mater. Sol. Cells* **2008**, *92*, 727.

[4] P. Vanlaeke, G. Vanhoyland, T. Aernouts, D. Cheyns, D. Deibel, J. V. Manca, P. Heremans, J. Poortmans, *Thin Solid Films* **2006**, *511–512*, 358.

[5] V. D. Mihailetchi, H. Xie, B. de Boer, L. J. A. Koster, P. W. M. Blom, *Adv. Funct. Mater.* **2006**, *16*, 699.

[6] H. Bässler, *Phys. Status Solidi B* **1993**, *175*, 15.

[7] C. Tanase, E. J. Meijer, P. W. M. Blom, D. M. de Leeuw, *Phys. Rev. Lett.* **2003**, *91*, 216601.

[8] A. J. Mozer, N. S. Sariciftci, *Chem. Phys. Lett.* **2004**, *389*, 438.

[9] H. Sirringhaus, P. J. Brown, R. H. Friend, M. M. Nielsen, K. Bechgaard, B. M. W. Langeveld-Voss, A. J. H. Spiering, R. A. J. Janssen, E. W. Meijer, P. Herwig, D. M. de Leeuw, *Nature* **1999**, *401*, 685.

[10] A. Salleo, T. W. Chen, A. R. Völkel, Y. Wu, P. Liu, B. S. Ong, R. A. Street, *Phys. Rev. B* **2004**, *70*, 115311.

[11] H. Sirringhaus, *Adv. Mater.* **2005**, *17*, 2411.

[12] G. Garcia-Belmonte, A. Munar, E. M. Barea, J. Bisquert, I. Ugarte, R. Pacios, *Org. Electron.* **2008**, *9*, 847.

[13] G. Dicker, M. P. de Haas, L. D. A. Siebbeles, J. D. Warman, *Phys. Rev. B* **2004**, *70*, 045203.

[14] T. J. Savenije, J. E. Kroeze, M. M. Wienk, J. M. Kroon, J. D. Warman, *Phys. Rev. B* **2004**, *69*, 155205.

[15] P. A. C. Quista, T. Martens, J. V. Mancab, T. J. Savenije, L. D. A. Siebbeles, *Sol. Energy Mater. Sol. Cells* **2006**, *90*, 362.

[16] A. J. Ferguson, N. Kopidakis, S. E. Shaheen, G. Rumbles, *J. Phys. Chem. C* **2008**, *112*, 9865.

[17] G. Dicker, M. P. de Haas, J. M. Warman, D. M. de Leeuw, L. D. A. Siebbeles, *J. Phys. Chem. B* **2004**, *108*, 17818.

[18] G. Dicker, M. P. de Haas, D. M. de Leeuw, L. D. A. Siebbeles, *Chem. Phys. Lett.* **2005**, *402*, 370.

[19] M. P. de Haas, J. M. Warman, T. D. Anthopoulos, D. M. de Leeuw, *Adv. Funct. Mater.* **2006**, *16*, 2274.

[20] M. Kunst, A. Werner, *J. Appl. Phys.* **1985**, *58*, 2236.

[21] J. Orenstein, M. Kastner, *Phys. Rev. Lett.* **1981**, *46*, 1421.

[22] J. Orenstein, M. Kastner, V. Vaninov, *Philos. Mag. B* **1982**, *46*, 23.

[23] H. Sirringhaus, P. J. Brown, R. H. Friend, M. M. Nielsen, K. Bechgaard, B. M. W. Langeveld-Voss, A. J. H. Spiering, R. A. J. Janssen, E. W. Meijer, P. Herwig, D. M. de Leeuw, *Nature* **1999**, *401*, 685.

[24] E. A. Schiff, *Phys. Rev. B* **1981**, *24*, R6189.

[25] C. Im, H. Bässler, H. Rost, H. H. Hörhold, *J. Chem. Phys.* **2000**, *113*, 3802.

[26] P. M. Borsenberger, L. Pautmeier, H. Bässler, *J. Chem. Phys.* **1991**, *94*, 5447.

[27] A. J. Mozer, G. Dennler, N. S. Sariciftci, M. Westerling, A. Pivrikas, R. Österbacka, G. Juska, *Phys. Rev. B* **2005**, *72*, 035217.

[28] I. Montanari, A. F. Nogueira, J. Nelson, J. R. Durrant, C. Winder, M. A. Loi, N. S. Sariciftci, C. Brabec, *Appl. Phys. Lett.* **2002**, *81*, 3001.

[29] A. F. Nogueira, I. Montanari, J. Nelson, J. R. Durrant, C. Winder, Sariciftci, C. Brabec, *J. Phys. Chem. B* **2003**, *107*, 1567.

[30] O. Rubel, W. Stolz, S. D. Baranovskii, *Appl. Phys. Lett.* **2007**, *91*, 021903.

[31] V. Kytin, H. E. Porteanu, O. Loginenko, T. Dittrich, *Phys. Status Solidi A* **2003**, *197*, 257.

[32] A. Werner, M. Kunst, *Phys. Rev. B* **1987**, *36*, 7567.

[33] C. Swiatkowski, A. Sanders, K.-D. Buhre, M. Kunst, *J. Appl. Phys.* **1995**, *78*, 1763.